Interdisciplinary Research in Medical Sciences Specialty
ISSN: 3062-4401
2023, Volume 3, Issue 1, Page No: 58-70

Available online at: www.galaxypub.co/page/journals

Galaxy Publication

Exploring the Role of Unani Medicine in Managing Nisyan (Dementia): In Vitro and Ex Vivo Study of a Lavandula stoechas L. (Ustukhuddu¯s)–Loaded Unani Transdermal Patch

Amir Khalil[1], Samir Dawoud[1], Hassan Youssef[1]*

[1]Department of Biomedical Engineering, Faculty of Medicine, American University of Beirut, Beirut, Lebanon.

***E-mail** ✉ hassan.youssef.bio@outlook.com

Received: 16 October 2022; **Revised:** 28 January 2023; **Accepted:** 05 February 2023

ABSTRACT

Lavandula stoechas L. (Ustukhuddūs) has long been employed in traditional medicine for managing neurological conditions such as dementia, yet conventional oral and topical formulations often fail to achieve optimal therapeutic effects. To overcome these limitations, this study developed matrix-type transdermal patches incorporating Ustukhuddūs hydro-alcoholic extract (UHAE) and essential oil (UEO) using a combination of hydrophilic hydroxyl propyl methyl cellulose (HPMC) and hydrophobic ethyl cellulose (EC) polymers. Comprehensive characterization through ATR–FTIR, DSC, XRD, and SEM confirmed the compatibility of the bioactive components with the polymer matrix and verified successful patch formation. The patches were evaluated for physicochemical properties, in vitro drug release, and ex vivo skin permeation. Findings demonstrated that the films were uniform, smooth, transparent, flexible, and non-irritant. Sustained drug release was observed, with UHAE and UEO patches releasing 81.61 % and 85.24 % of their payload, respectively, following non-Fickian kinetics. Ex vivo studies further revealed drug permeation of 66.82 % for UHAE and 76.41 % for UEO. These results indicate that the formulated patches are effective TDDS candidates, offering enhanced patient compliance and highlighting the potential of Unani medicine in the therapeutic management of Nisyan (dementia).

Keywords: Skin irritation, Ex vivo permeation, Sustained-release, Essential oil, Unani transdermal patch, Ustukhuddūs

How to Cite This Article: Khalil A, Dawoud S, Youssef H. Exploring the Role of Unani Medicine in Managing Nisyan (Dementia): In Vitro and Ex Vivo Study of a Lavandula stoechas L. (Ustukhuddu¯s)–Loaded Unani Transdermal Patch. Interdiscip Res Med Sci Spec. 2023;3(1):58-70. https://doi.org/10.51847/BMS7yIMnCQ

Introduction

A drug delivery system (DDS) refers to a collection of physicochemical strategies designed to regulate the administration and release of pharmacologically active compounds into cells, tissues, and organs, thereby maximizing their therapeutic effects. Delivery methods vary depending on the chosen route of administration, among which the transdermal drug delivery system (TDDS) has emerged as a particularly appealing approach, garnering considerable attention from researchers worldwide. Recently, TDDS has gained recognition as a promising alternative to oral and injectable routes due to its painless, convenient application, potential to enhance drug bioavailability, and minimal burden on patients [1, 2]. Additional advantages of TDDS include bypassing the gastrointestinal tract and avoiding first-pass hepatic metabolism. However, the full potential of TDDS is often limited by the inherent barrier properties of the skin. Transdermal patches are drug-containing adhesive systems designed to deliver medication through the skin layers into systemic circulation at a controlled rate [3]. Widely used for various medical conditions, these patches offer controlled drug release, ensuring steady systemic levels [4, 5]. They are advantageous due to their ease of preparation, user-friendly application, capacity to accommodate both hydrophilic and lipophilic drugs, and improved stability for long-term dermal delivery. Importantly, transdermal patches provide consistent and controlled drug release, preventing abrupt fluctuations in plasma drug

concentrations and supporting better adherence to prescribed regimens [4, 6]. This approach is particularly beneficial for patients requiring long-term therapy or those unable or unwilling to take oral medications [7, 8].

Neuropsychiatric disorders, such as depression, attention deficit hyperactivity disorder (ADHD), Parkinson's disease (PD), and dementia, often necessitate prolonged medication, which can lead to poor compliance, treatment discontinuation, and increased caregiver burden. Long-acting formulations are advantageous in these cases because they maintain stable drug levels, offering consistent symptom management rather than intermittent peaks in plasma concentration. Evidence indicates that sustained anti-dementia therapy at appropriate doses slows cognitive decline, reduces the need for institutional care, and lowers overall healthcare costs [9, 10]. Due to noncompliance and adverse effects associated with orally administered cholinesterase inhibitors in dementia, TDDS has been developed for various agents, including tacrine, physostigmine, and phenserine tartrate; however, the only commercially available transdermal acetylcholinesterase inhibitor is the rivastigmine patch (Exelon® Patch) [9, 10]. The rivastigmine patch provides sustained drug release, maintains steady plasma concentrations, and is appreciated for ease of use and minimal disruption to daily activities [11–13].

Ustukhuddūs (Lavandula stoechas L., Lamiaceae), a well-known remedy in Unani Medicine, is used for multiple neurological conditions including epilepsy, catalepsy, dementia, insanity, mental weakness, and obsessive thoughts, earning the epithet "Broom of the brain" for its cognitive tonic properties [14, 15]. Its extracts and essential oils exhibit a range of pharmacological activities, including hypnotic [16], nootropic [17], anticonvulsant, sedative, antispasmodic [18], anti-apoptotic [19], antioxidant, and anti-inflammatory effects [20]. Traditional Unani practices recommend both oral intake and topical application of Ustukhuddūs paste on the head for conditions like dementia and catalepsy [15]. Despite its therapeutic potential, oral administration is limited by low bioavailability, bulkiness, and frequent dosing requirements, while the paste form suffers from inconsistent dosing, incomplete drug release, and challenges in patient adherence [21].

To address these limitations, developing polymer-based transdermal patches of Ustukhuddūs represents a promising solution, offering controlled drug release and improved patient compliance. This study is the first to focus on formulating transdermal patches incorporating hydro-alcoholic extracts and essential oils of Ustukhuddūs using a combination of hydrophilic and hydrophobic polymers. The study also evaluates the patches' in vitro and ex vivo permeation characteristics alongside their sustained release profile.

Materials and Methods

Materials

Hydroxypropyl methylcellulose (HPMC) was obtained from High Purity Laboratory Chemicals Pvt. Ltd., Mumbai. Ethyl cellulose, dibutyl phthalate (DBP), dimethyl sulfoxide (DMSO), and methanol were procured from Thomas Baker Chemicals Pvt. Ltd., Ambernath. Ethanol was supplied by Jiangyin Import & Export Co. Ltd., China, while chloroform and dichloromethane were purchased from Nice Chemicals Pvt. Ltd., Kochi and Sisco Research Laboratories, Maharashtra, respectively. Glycerine was sourced from SD Fine Chemicals Ltd., Mumbai. All chemicals and solvents used were of analytical grade.

Methods

Extraction of ustukhuddūs and essential oil

Dried aerial parts of Ustukhuddūs (Lavandula stoechas L.) were procured from Green Earth Products Pvt. Ltd., New Delhi, and authenticated at the Drug Standardisation and Research Unit (DSRU), Regional Research Institute of Unani Medicine (RRIUM), Chennai. A specimen was deposited at the Drug Museum, National Institute of Unani Medicine (NIUM), Bengaluru (voucher no. 115/1S/Res/2022). The extraction was performed following the procedure of Mustafa SB, 2019 [21]. In brief, 20 g of coarsely powdered plant material was soaked in a 50% hydro-alcoholic solution (water: ethanol, 1:20 w/v) and continuously agitated on a rotary shaker for 72 hours. The mixture was filtered initially through muslin cloth and then re-filtered using Whatman filter paper. The extraction was repeated three times, and all filtrates were combined. The pooled filtrate was concentrated under reduced pressure using a rotary evaporator at 40 °C and 90 rpm. The residue was further dried in a vacuum oven at 40 °C, weighed, and the extraction yield was calculated relative to the initial plant material. The dried extract was stored in airtight containers at −4 °C for subsequent use [22]. Essential oil was obtained via steam distillation using a Clevenger apparatus as described by Al-Mariri, 2013 [23].

Development of ustukhuddūs transdermal patches

Transdermal patches were formulated based on the solvent casting method reported by Patel N A, 2009 [24]. Two types of matrix patches were prepared using Ustukhuddūs hydro-alcoholic extract (UHAE) and essential oil (UEO) combined with hydrophilic HPMC K4M (100 mg) and hydrophobic ethyl cellulose (EC, 25 mg). Polymers were dissolved in a solvent mixture of chloroform, methanol, and dichloromethane in a ratio of 2:2:1. The calculated amount of UHAE or UEO was dispersed into the polymer solution with thorough mixing to ensure uniform drug distribution. Dibutyl phthalate (DBP) was added at 30% of the total polymer weight as a plasticizer, and dimethyl sulfoxide (DMSO) was included at 20% of polymer weight as a permeation enhancer (**Table 1**). The prepared mixture was poured into glycerine-lubricated square molds and left to dry at ambient temperature under an inverted funnel to minimize dust contamination. After 24 hours, the dried patches were cut into 1 cm^2 pieces, wrapped in aluminum foil, and stored in a desiccator. Drug-free patches were prepared similarly to serve as blanks [24].

Table 1. Composition of UEO, UHAE, and blank blended patches[a].

Patch	Amount of drug (mg)	Polymer		Plasticizer	Permeation Enhancer	Solvent (v/v) mL
		HPMC (mg)	EC (mg)	DBP (mg)	DMSO (mg)	Chl:MeOH:DCM
UEO	25	100	25	37.5	25	2:2:1
UHAE	54	100	25	37.5	25	2:2:1
Blank	–	100	25	37.5	25	2:2:1

aHPMC indicates hydroxyl propyl methyl cellulose; EC, ethyl cellulose; DBP, dibutyl phthalate; DMSO, dimethyl sulfoxide; Chl, chloroform; MeOH, Methanol; DCM, Dichloromethane; UHAE, Ustukhuddūs hydro-alcoholic extract; UEO, Ustukhuddūs essential oil.

Drug-polymer compatibility and interaction studies

ATR-FTIR spectroscopy

The potential interactions between the active components and polymer matrices were examined using ATR-FTIR on a PerkinElmer Spectrum-1 FTIR spectrometer (PerkinElmer, USA) according to Suksaeree J, 2015 [25]. Spectra were recorded for pure HPMC, EC, blank patches, and patches containing UHAE or UEO. Characteristic functional group peaks were identified across a wavenumber range of 500–4000 cm^{-1} with a resolution of 4 cm^{-1} to detect any chemical incompatibility.

Differential Scanning Calorimetry (DSC)

Thermal properties and ingredient compatibility were assessed using DSC (Netzsch DSC 204, Germany) as described by Suksaeree J, 2015 [25]. Samples were sealed in hermetic pans and heated from 20 to 350 °C at a rate of 10 °C/min under a nitrogen atmosphere. Endothermic events and thermograms were recorded to evaluate potential interactions and stability of the formulations.

X-Ray Diffraction (XRD)

Crystallinity and compatibility within the polymer matrices were studied using XRD on a D8 Advance Bruker diffractometer (Singapore), following Suksaeree J, 2015 [25]. Blank patches, UHAE patches, and UEO patches were scanned at 40 kV and 45 mA across a 2θ range of 5–40° with a step size of 0.02°/s to analyze structural changes or interactions.

Scanning Electron Microscopy (SEM)

Surface and cross-sectional morphology were examined using SEM (FEI Quanta 200, MK II, USA). Samples, incubated at 37 °C on glass slides, were observed under high vacuum with an accelerating voltage of 20 kV using the Everhart-Thornley detector, enabling evaluation of patch surface uniformity and structural integrity [25].

Physicochemical evaluation of patches

Visual inspection

Each patch was inspected for color, transparency, smoothness, flexibility, and uniformity, including the absence of air bubbles, according to Latif MS, 2021 [26]. Patches with visible flaws, uneven thickness, or irregular weights were excluded from further testing.

Weight assessment

The weight of each patch was individually measured using an analytical balance (Shimadzu AX 200, Kyoto, Japan) and compared against the mean weight of the batch to ensure consistency [26].

Thickness evaluation

Patch thickness was measured at six different points using a vernier caliper, and the mean thickness was calculated to verify uniformity [26].

Drug loading

The content of UHAE and UEO in the patches was quantified using a UV–visible spectrophotometer (Shimadzu 1601, Kyoto, Japan) at 273 nm and 278 nm, respectively, following appropriate dilution, as described by Latif MS, 2021 [26].

Folding endurance

The ability of patches to withstand repeated folding was tested to assess plasticizer effectiveness. Each patch was folded at the same spot until cracks appeared, in accordance with Latif MS, 2021 [26].

Moisture uptake

Moisture absorption was evaluated by exposing the patches to a humid environment and measuring the weight difference before and after exposure. The percent moisture uptake was calculated for each patch, and averages were reported [26].

Moisture content

Patch moisture content was determined using the method of Latif MS, 2021 [26], with the following formula:

$$\%\ Moisture\ Loss\ =\ (wi\ -\ wf)/wi\ \times \quad (1)$$

Where wi is the initial patch weight, and wf is the final patch weight.

Surface pH

The surface pH of the prepared transdermal patches was evaluated according to the procedure described by Latif MS, 2021 [26] using a pH meter (InoLab®, Xylem Analytics, Germany).

Percent elongation at break

The elongation capacity of each patch was determined by measuring its length immediately before rupture. Percent elongation was calculated using the formula:

$$\%\ Elongation\ =\ (L_1\ -\ L_2)/L_2\ \times\ 10 \quad (2)$$

Where L_1 is the final patch length before breaking, and L_2 is the initial patch length.

Flatness

The flatness of the patches was assessed according to the procedure outlined by Singh A, 2016 [27], and was determined using the specified equation:

$$\%\ Constriction\ =\ =\ (L_1\ -\ L_2)/L_1\ \times\ 100 \quad (3)$$

Where L_1 is the initial strip length, and L_2 is the strip length.

Skin irritation study

The potential of the developed patches to induce skin irritation or sensitization was evaluated using hypersensitivity tests on rat skin. Healthy male Wistar albino rats, weighing 200–250 g, were obtained from a registered breeder in Bengaluru, and all experiments were conducted in the Animal House at the National Institute of Unani Medicine, Bengaluru. Ethical approval was granted by the Institutional Animal Ethics Committee

(IAEC) under No. IAEC/6/19/IA/07. Skin irritation was assessed using the Draize patch test [26], with two groups of six rats each employed to test each formulation. The hypersensitivity evaluation of UHAE, UEO, and blank patches followed the method described by Latif MS, 2021 [26], using a visual scoring system: 0 indicated no irritation, 1 slight irritation, 2 well-defined irritation, 3 moderate irritation, and 4 represented scar formation [26].

In vitro drug release study

In vitro release profiles of UHAE and UEO patches were determined using a modified Franz diffusion cell with an eggshell membrane, following the method of Baviskar DT, 2013. Drug content in UHAE and UEO patches was measured spectrophotometrically at 273 nm and 278 nm, respectively, after appropriate dilution with phosphate buffer (pH 7.4), and all tests were performed in triplicate [28].

Kinetics of drug release

Drug release patterns of all batches were fitted to various mathematical models—including Zero-order, First-order, Higuchi, Hixson-Crowell, Korsmeyer-Peppas, Hopfenberg, Weibull, Makoid-Banakar, Baker-Lonsdale, and Peppas-Sahlin—to determine release kinetics [26]. Correlation coefficients and rate constants were calculated using the DD Solver Add-In [29].

Ex vivo permeation study

Ex vivo permeation of UHAE and UEO patches was assessed using a modified Franz diffusion cell with pig flank skin as the membrane, following Baviskar DT, 2013. The pig skin was obtained from a local slaughterhouse where animals were slaughtered for human consumption, with no animals sacrificed specifically for this study. Drug content was measured spectrophotometrically at 273 nm and 278 nm, following suitable dilution with fresh medium. Each experiment was conducted in triplicate, and cumulative drug permeation (μg/cm²) was plotted against time [28].

Skin penetration study

The amount of drug retained within the skin from UHAE and UEO patches was assessed according to Salemo C, 2010 [30]. Skin penetration was calculated as the difference between the total applied dose and the sum of the permeated drug and the residual amount on the skin.

Statistical analysis

All experiments were performed in triplicate, with results expressed as mean ± standard deviation.

Results and Discussion

Organoleptic properties of ustukhuddūs extract, essential oil, and developed patches

The yields of UHAE and UEO were 30% and 0.4% (g/g), respectively. UHAE appeared greenish-dark brown, highly sticky, intensely bitter, and strongly aromatic, whereas UEO was dark yellow, strongly bitter, and possessed a potent camphor-like aroma. Blank patches were white, while patches containing UHAE and UEO were dark brown and pale yellow, respectively, reflecting their constituents. The developed transdermal patches, formulated with suitable polymers and excipients, exhibited smooth, clear, homogeneous films without air bubble entrapment.

Drug-polymer interaction and compatibility studies

FTIR spectra of HPMC, EC, UHAE, and UEO patches were analyzed **(Figure 1)**. HPMC showed characteristic peaks at 3448 cm^{-1} (–OH stretching), 2897 and 2096 cm^{-1} (C–H stretching), 1640 cm^{-1} (C–O stretching), 1375 cm^{-1} (C–O–C stretching), and 1051 cm^{-1} (C–O stretching) **(Figure 1A)**. EC displayed peaks at 3469 cm^{-1} (–OH stretching), 2967 and 2867 cm^{-1} (C–H stretching), 1367 cm^{-1} (C–O–C stretching), and 1050 cm^{-1} (C–O stretching) **(Figure 1B)**. The UHAE patch exhibited peaks at 3374 cm^{-1} (O–H stretching), 2933 cm^{-1} (C–H stretching), 1720 cm^{-1} (C=O stretching and bending), 1374 cm^{-1} (C–O–C stretching), 1278 cm^{-1} (C–O stretching), and 1048 cm^{-1} (C–H bending) **(Figure 1C)**. UEO patch peaks were at 3377 cm^{-1} (O–H stretching), 2936 cm^{-1} (C–H stretching), 1730 cm^{-1} (C=O stretching), 1374 cm^{-1} (C–O–C stretching), 1278 cm^{-1} (C–O stretching), and 1050 cm^{-1} (C–H bending) **(Figure 1D)**. The spectra indicated that drug peaks remained distinct alongside polymer peaks, confirming the drug's chemical stability and compatibility with the excipients.

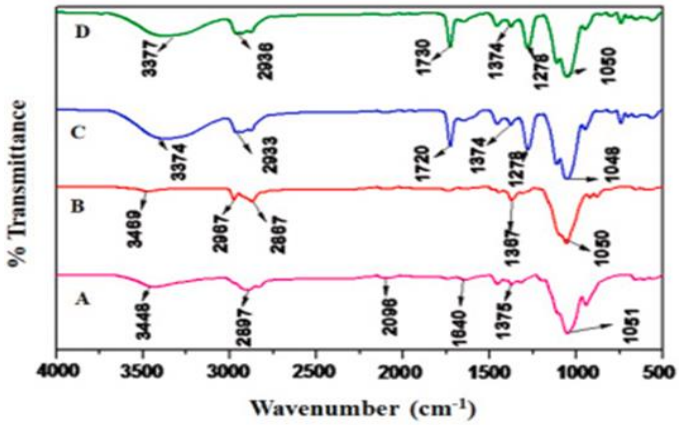

Figure 1. FTIR spectra of (A) HPMC, (B) EC, (C) UHAE patch, and (D) UEO patch*. *Abbreviations: HPMC, hydroxyl propyl methyl cellulose; EC, ethyl cellulose; UHAE, Ustukhuddūs hydro-alcoholic extract; UEO, Ustukhuddūs essential oil.

The thermal characteristics of UHAE- and UEO-incorporated patches were investigated using differential scanning calorimetry (DSC) [25]. The DSC profiles of pure UHAE, EC, HPMC, UEO, and UHAE-loaded patches are presented in **Figure 2**. Pure UHAE displayed four distinct endothermic events at 118.5 °C, 124.0 °C, 138.1 °C, and 146.6 °C, associated with its melting transitions, with a total enthalpy (ΔH) of 139.7 J/g **(Figure 2A)**. EC exhibited a broad endothermic transition at 55.9 °C (ΔH = −14.26 J/g) followed by an exothermic event at 194.9 °C (ΔH = −23.2 J/g) **(Figure 2B)**. HPMC showed a broad endothermic peak at 65.7 °C (ΔH = 124.8 J/g) and an exothermic peak at 268.7 °C (ΔH = −14.55 J/g), likely reflecting moisture loss **(Figure 2C).** The UEO patch revealed two endothermic peaks, the first at 82.4 °C (ΔH = 235.9 J/g) and a second at 235 °C (ΔH = 204.2 J/g) **(Figure 2D)**. In the UHAE-loaded patch, an initial broad endothermic peak appeared at 95.9 °C (ΔH = 379.6 J/g), followed by an exothermic peak at 237.3 °C (ΔH = 160.8 J/g) **(Figure 2E).**

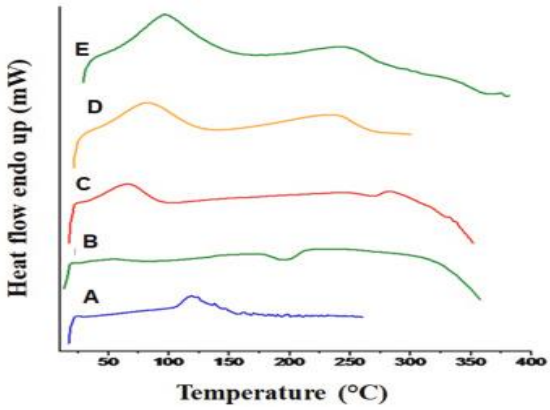

Figure 2. DSC thermograms of (A) crude hydro-alcoholic extract, (B) EC, (C) HPMC, (D) UEO patch, and (E) UHAE patch.

Analysis of the DSC data revealed that the characteristic endothermic peak of pure UHAE was absent in the UHAE-loaded patch, likely due to the successful incorporation of the extract into the HPMC and EC polymer matrix. The thermogram of the physical mixture closely mirrored that of the extract, indicating thorough dispersion of the active compound within the polymeric network and suggesting no chemical complexation occurred between the drug and the polymers. In both UHAE and UEO patch thermograms, no additional peaks or significant changes in peak shape and onset were detected. Slight shifts observed in the HPMC and EC peaks were attributed to residual moisture in the patch matrix. These results confirm the chemical stability of the patches and the absence of any interactions between the active ingredients and the polymers.

X-Ray Diffraction (XRD) analysis

The XRD patterns of blank, UHAE-, and UEO-loaded patches are presented in **Figure 3**. XRD was employed to evaluate drug–polymer compatibility and to distinguish crystalline versus amorphous structures in the formulations [25]. Blank patches composed of HPMC and EC displayed a diffraction peak near 20.92°, consistent with semi-crystalline characteristics. In contrast, patches containing UHAE or UEO exhibited broad halos characteristic of amorphous material. The disappearance of the original HPMC and EC crystalline peaks in these drug-loaded patches suggests that the active compounds were uniformly dispersed within the polymer matrix, further supporting the compatibility of the developed formulations.

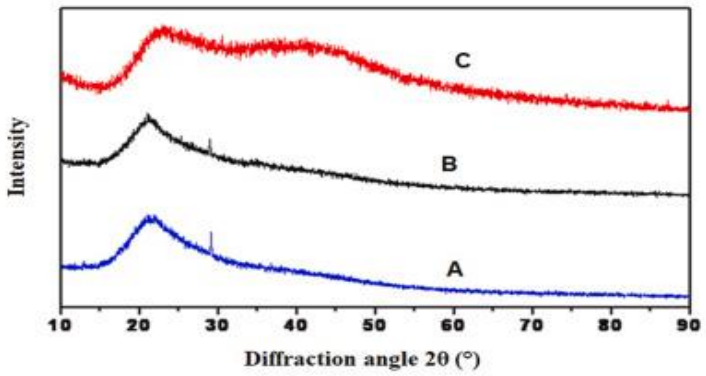

Figure 3. X-ray diffraction patterns of the UHAE patch (A), blank patch (B), and UEO patch (C), where UHAE stands for Ustukhuddūs hydro-alcoholic extract and UEO for Ustukhuddūs essential oil.

High-resolution SEM images of the patch surfaces and cross-sections **(Figure 4)** showed that blank patches had a consistently smooth and dense appearance with no visible pores. In contrast, incorporating crude UHAE or UEO into the patches resulted in surfaces that were irregular and coarse, likely due to the formation of dispersed clusters and aggregates of the extracts within the patch matrix.

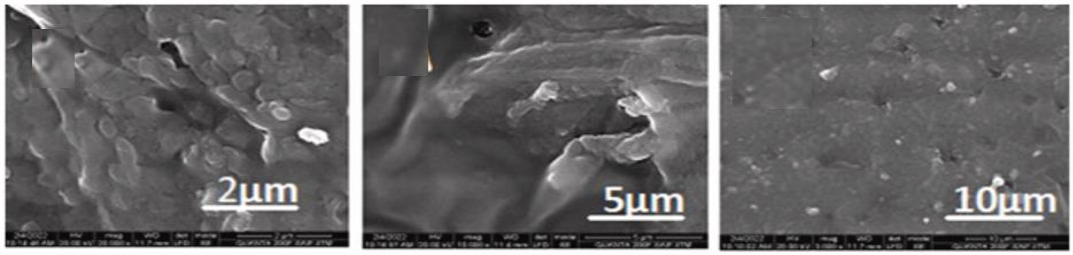

a)

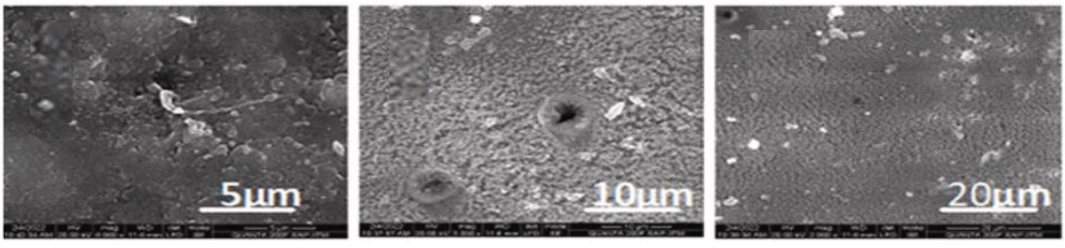

b)

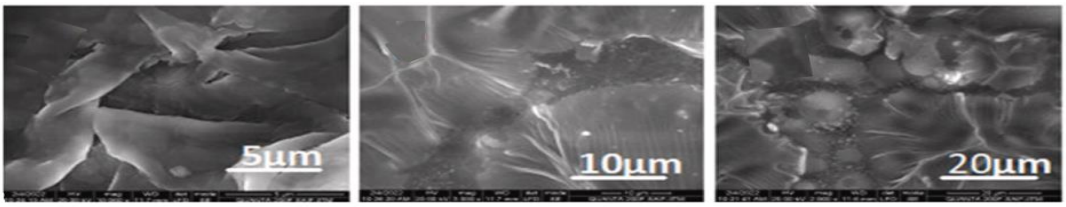

c)

Figure 4. Representative SEM images of (a) blank patch, (b) UHAE patch, and (c) UEO patch, where UHAE refers to Ustukhuddūs hydro-alcoholic extract and UEO to Ustukhuddūs essential oil.

Physicochemical evaluation of formulated patches

The physicochemical properties of the blank, UHAE, and UEO-incorporated patches are summarized in **Table 2.** The average weight of the blank, UHAE, and UEO patches was 53.51 ± 1.230 mg, 70.256 ± 2.009 mg, and 58.486 ± 0.217 mg, respectively, while their mean thicknesses were 0.31 ± 0.02 mm, 0.436 ± 0.015 mm, and 0.31 ± 0.017 mm. Weight uniformity and thickness variation across the different patches were within acceptable limits. The low standard deviation values indicate that the patches were uniform and that the preparation method was reproducible. The mean drug content for UHAE and UEO patches was determined to be 83.94 ± 1.12% and 85.49 ± 0.67%, respectively, reflecting consistent drug loading and even distribution throughout the patches.

Folding endurance is a key quality parameter for transdermal patches, as higher values reflect greater resistance to breakage or damage [31]. In this study, folding endurance was measured as 42.666 ± 4.041, 26.293 ± 0.577, and 49.333 ± 3.511 for blank, UHAE, and UEO patches, respectively. These results indicate satisfactory flexibility for all patches, with the UHAE patch showing slightly lower flexibility, likely due to its higher moisture content.

Table 2. Physicochemical properties of Formulated Patches (n = 3).
All values are expressed as mean ± SD (*n* = 3). UHAE indicates Ustukhuddūs hydro-alcoholic extract; UEO, Ustukhuddūs essent ial oil.

Parameters	Formulations		
	UHAE patch	**UEO Patch**	**Blank Patch**
Weight Uniformity (mg)	70.256 ± 2.009	58.486 ± 0.217	53.51 ± 1.230
Drug Content (%)	83.94 ± 1.12	85.49 ± 0.67	–
Thickness (mm)	0.436 ± 0.015	0.31 ± 0.017	0.31 ± 0.02
Folding Endurance (no's)	26.293 ± 0.577	49.333 ± 3.511	42.666 ± 4.041
Moisture Uptake (%)	2.983 ± 0.120	2.18 ± 0.055	2.383 ± 0.070
Surface pH	5.726 ± 0.073	5.17 ± 0.088	5.903 ± 0.023
Moisture Content (%)	3.186 ± 0.083	2.786 ± 0.070	2.846 ± 0.111
Percentage Elongation (%)	17.666 ± 4.041	37.666 ± 4.041	35.33 ± 4.041
Flatness (%)	100	100	100

The moisture uptake of the formulated patches was measured as 2.383 ± 0.070% for the blank patch, 2.983 ± 0.120% for the UHAE patch, and 2.18 ± 0.055% for the UEO patch, while their moisture content was found to be 2.846 ± 0.111%, 3.186 ± 0.083%, and 2.786 ± 0.070%, respectively. Both parameters were within acceptable limits. The relatively low moisture uptake helps prevent microbial contamination and reduces the bulkiness of the patches, whereas the low moisture content enhances stability and reduces brittleness [28]. Surface pH values for the blank, UHAE, and UEO patches were 5.903 ± 0.023, 5.726 ± 0.073, and 5.17 ± 0.088, respectively, remaining in a safe range that indicates minimal risk of skin irritation or sensitization [26].

The patches' flexibility, expressed as percentage elongation, was 35.33 ± 4.041% for blank, 17.666 ± 4.041% for UHAE, and 37.666 ± 4.041% for UEO patches. For transdermal applications, sufficient elasticity is critical to allow patches to conform to skin movements without cracking or breaking, and these results indicate that blank and UEO patches possess superior flexibility compared to UHAE patches. All patches displayed 100% flatness, with no change in strip length after longitudinal cuts, demonstrating that the patches maintain a smooth and uniform surface upon application [27].

Skin irritation study

When applied to healthy male Wistar rats for 24 hours, neither UHAE nor UEO patches induced any edema or erythema at the application sites. These findings confirm that both formulations are non-irritating and safe for transdermal use.

In vitro drug release study

Evaluating drug release profiles is crucial for controlled-release systems, as it ensures a constant and predictable drug permeation rate. Maintaining a higher concentration of the drug on the surface of the stratum corneum compared to systemic levels is essential for achieving controlled-release performance. In this study, the in vitro release of UHAE and UEO patches—containing 54 mg/cm² of extract and 25 mg/cm² of essential oil, respectively—was assessed using Franz diffusion cells with an eggshell membrane model, which closely resembles human stratum corneum. The release profile exhibited a pronounced initial burst within the first 7 hours, followed by a gradual approach to a plateau, reflecting sustained-release behavior of the patch matrices over 24 hours. The cumulative drug release after 24 hours was 81.61 ± 0.37% for UHAE and 85.24 ± 0.42% for UEO patches **(Figure 5)**. The rapid initial release observed during the first 7 hours is likely due to the swift diffusion of the drug from the patch surface into the receptor medium. The overall controlled-release behavior of these patches is particularly promising for chronic conditions such as dementia, as they can maintain stable plasma drug concentrations and serve as effective long-acting formulations.

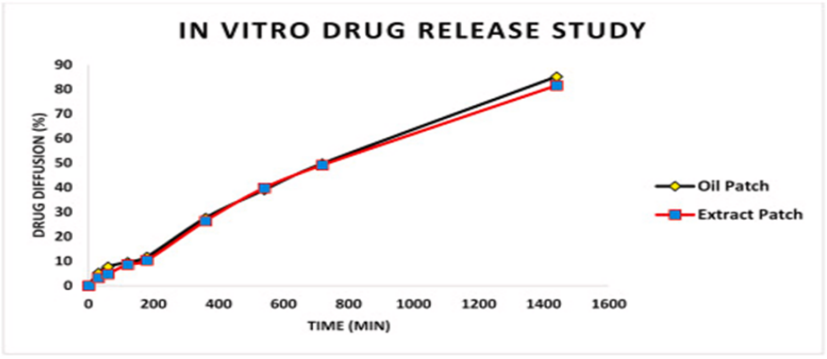

a)

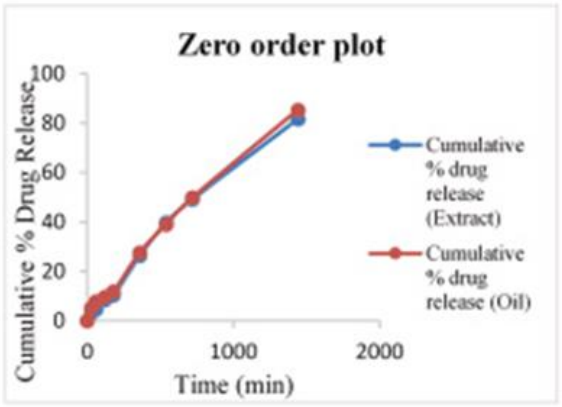

b)

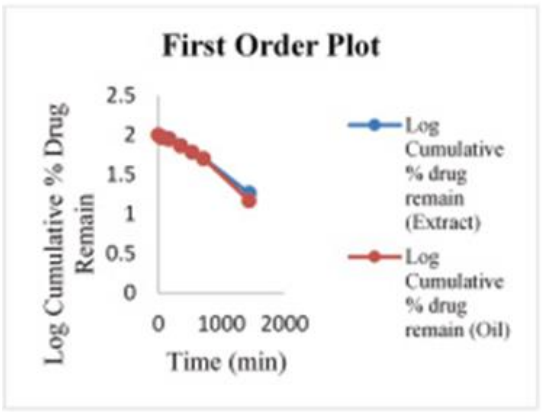

c)

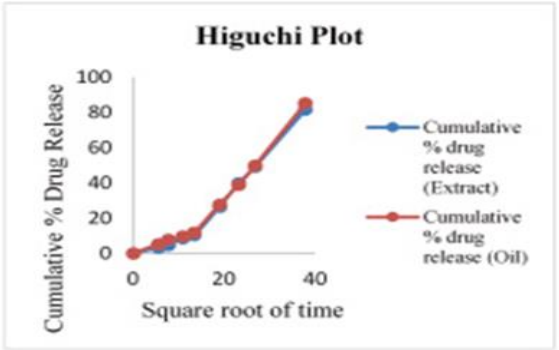

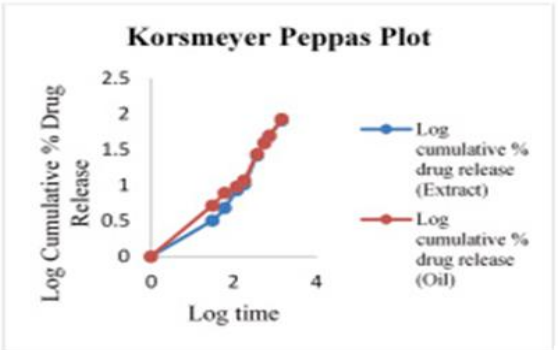

d) e)

Figure 5. In vitro drug release profiles of the optimized patches, along with the release kinetics analyzed using zero-order, first-order, Higuchi, and Korsmeyer–Peppas models. Here, "oil patch" refers to the Ustukhuddūs essential oil patch, while "extract patch" refers to the Ustukhuddūs hydro-alcoholic extract patch. All values are presented as mean ± SD (n = 3).

Analysis of moisture uptake and SEM-based porosity suggests that HPMC polymers likely created significant free volume within the drug-loaded patches. This increased molecular mobility and segmental relaxation, facilitating enhanced drug diffusion. The presence of an amorphous region within the matrix-type patches further contributed to improved drug release [32]. Both UHAE and UEO patches exhibited sustained drug release; however, the cumulative release from the UHAE patch was notably lower than that of the UEO patch. This enhanced release from the UEO patch can be attributed to the essential oil and its volatile constituents, which are known to act as effective penetration enhancers [33].

Drug release kinetics

The drug release patterns from UHAE and UEO patches were evaluated using various mathematical models, as presented in **Table 3** and **Figure 5**. Regression analysis indicated that the Weibull model best described the release behavior of both patches, with R^2 values of 0.9985 for UHAE and 0.9967 for UEO. The Korsmeyer–Peppas model yielded n values between 0.5 and 1 for both formulations, indicating a non-Fickian release mechanism. This suggests that drug release from the patches occurs through a combination of diffusion and matrix erosion/swelling, demonstrating controlled and sustained delivery characteristics.

Table 3. Regression parameters of formulated patches after fitting the drug release data to various release kinetic models.

All values are expressed as mean ± SD (*n* = 3).

Mathematical models	Essential oil Patch	Extract Patch
Zero- order Model	0.9893	0.9826
R^2 k_0 (h^{-1})	0.063	0.061
First – Order Model	0.9790	0.986
R^2 k_1 (h^{-1})	0.001	0.001
Higuchi Model	0.9452	0.9481
R^2 k_H($h^{-1/2}$)	1.841	1.777
Korsmeyer – Peppas Model	0.9962	0.9931
R^2	0.208	0.192
K_{kp}(h^{-n}) n	0.828	0.835
Hixson- Crowell Model	0.9922	0.9956
R^2 kHC	0.000	0.000
Hopfenberg Model	0.9963	0.9975
R^2	0.000	0.000
Khb n	1.700	1.934
Baker – Lonsdale Model	0.8455	0.8404
R^2 kBL	0.000	0.000
Makoid- Banakar Model	0.9966	0.9982
R^2 k_{MB}	0.126	0.034
N	0.921	1.153
k	0.000	0.000
Weibull Model		
R^2	0.9967	0.9985
A	32508.582	7636.136
B	1.500	1.298
Ti	−95.913	−26.001

Peppas- Sahlin Model	0.9962	0.9955
R^2 k1	−0.078	−2.272
k2	0.229	0.845
m	0.409	0.334

Ex vivo permeation study

Studying drug permeation through ex vivo skin is essential for predicting possible adverse effects and linking drug behavior to its in vivo pharmacokinetic profile. In this experiment, the cumulative amounts of drug that passed through the skin (µg/cm²) were recorded over time and plotted **(Figure 6)**. Newborn pig skin, which closely mimics human skin, was used as the barrier in a modified Franz diffusion cell to evaluate the permeation of UHAE and UEO patches. After 24 hours, the average cumulative permeated drug for the UHAE patch was 35,956 ± 0.24 µg/cm² (66.82 ± 1.74%), while the UEO patch reached 19,001 ± 1.46 µg/cm² (76.41 ± 1.22%), with the UEO patch showing significantly higher permeation than UHAE.

The faster initial permeation can be attributed to the rapid hydration and dissolution of the hydrophilic polymer HPMC when the patch contacts the skin, resulting in a high concentration of drug molecules at the skin surface. The presence of permeation enhancers further promotes the release of the drug from both hydrophilic and hydrophobic polymer components. In the later stages, the hydrophobic co-polymer EC regulates the release, producing a sustained drug delivery effect. These findings demonstrate that both UHAE and UEO patches can maintain therapeutic drug levels over 24 hours, although full release of the incorporated drug was not achieved within this period.

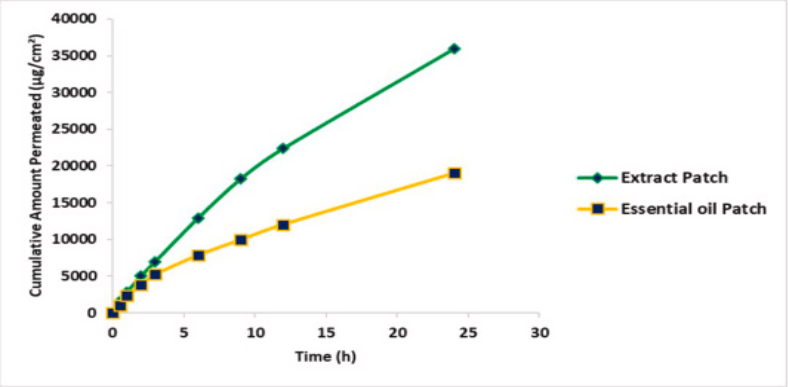

Figure 6. Ex vivo skin permeation profile of the optimized patches. The "extract patch" represents the Ustukhuddūs hydro-alcoholic extract patch, while the "essential oil patch" represents the Ustukhuddūs essential oil patch. All results are presented as mean ± SD (n = 3).

Skin penetration study

The skin penetration study revealed that the residual amounts of UHAE and UEO retained in the stratum corneum of pig skin were 26.06 ± 1.81% and 18.96 ± 1.35%, respectively. These findings suggest that the developed patches could potentially maintain drug availability for more than 24 hours, reducing the need for frequent application.

Conclusion

This study demonstrated the successful development of Unani transdermal patches incorporating Ustukhuddūs extract and essential oil, representing an important advancement from traditional Ḍimād (paste) formulations. The patches exhibited favorable physicochemical compatibility, physical stability, non-irritating properties, and sustained drug release, supporting their safety for potential human use. Among the formulations, the Ustukhuddūs essential oil patch showed superior performance compared to the extract patch in terms of physicochemical characteristics, drug release, and skin permeation. To the best of our knowledge, this is the first study reporting the effective formulation of Ustukhuddūs into transdermal patches, highlighting advantages over conventional dosage forms while maintaining sustained-release properties. Despite these promising results, further preclinical and clinical studies are necessary to confirm the therapeutic potential of these patches, particularly for dementia and other neurodegenerative disorders, and to fully explore the benefits of Ustukhuddūs in transdermal drug delivery.

Acknowledgments: MSK acknowledges the generous support from the Research Supporting Project (RSP2024R352), by the King Saud University, Riyadh, Saudi Arabia. A.S. is grateful to Ajman University, UAE for supporting this publication. The authors also acknowledge Prof. Abdul Wadud, Director, National Institute of Unani Medicine, Bengaluru, for providing good facilities for successful completion of this work. Authors also extend thanks to Dr. Jaculin Raiza, and Dr. Vivek Ghate for their support and guidance in carrying out *in vitro* and *ex vivo* studies.

Conflict of Interest: None

Financial Support: None

Ethics Statement: Ethical clearance was obtained from the Institutional Animal Ethics Committee (IAEC) vide No. IAEC/6/19/IA/07, National Institute of Unani Medicine, Bengaluru, INDIA.

References

1. Ruby P, Pathak SM, Aggarwal D, Sharma R, Singh A, Kumar V. Critical attributes of transdermal drug delivery system (TDDS)–a generic product development review. Drug Dev Ind Pharm. 2014;40(11):1421-8.
2. Pires LR, Vinayakumar KB, Turos M, Miguel V, Gaspar J, Ferreira L. A perspective on microneedle-based drug delivery and diagnostics in paediatrics. J Pers Med. 2019;9(4):49.
3. Wong WF, Lim V, Chen Y, Lim HY, Poh SC, Tan YF. Recent advancement of medical patch for transdermal drug delivery. Medicina. 2023;59(4):778.
4. Al Hanbali OA, Khan H, Sarfraz RM, Arafat M, Ijaz S, Murtaza G. Transdermal patches: design and current approaches to painless drug delivery. Acta Pharm. 2019;69(2):197-215.
5. Prajapati ST, Patel CG, Patel CN, Patel DM, Patel GN, Patel RP. Formulation and evaluation of transdermal patch of repaglinide. ISRN Pharm. 2011;2011:651909.
6. Alkilani AZ, McCrudden MT, Donnelly RF, Alqahtani FY, Alenezi SK, Alshammari TM. Transdermal drug delivery: innovative pharmaceutical developments based on disruption of the barrier properties of the stratum corneum. Pharmaceutics. 2015;7(4):438-70.
7. Prausnitz MR, Mitragotri S, Langer R, Weaver JC, Barry BW, Williams AC. Current status and future potential of transdermal drug delivery. Nat Rev Drug Discov. 2004;3(2):115-24.
8. Shakeel F, Ramadan W, Shafiq S, Alanazi FK, Alsarra IA, Mohsin K. Nanoemulsions as vehicles for transdermal delivery of aceclofenac. AAPS PharmSciTech. 2007;8:E191-9.
9. Isaac M, Holvey C, Thomas J, Kuruvilla K, Joseph A, Mathew B. Transdermal patches: the emerging mode of drug delivery system in psychiatry. Ther Adv Psychopharmacol. 2012;2(6):255-63.
10. Sadeghi M, Ghorbani A, Soleimani M, Ebrahimzadeh MA, Akbari J, Valizadeh H. Preparation and characterization of rivastigmine transdermal patch based on chitosan microparticles. Iran J Pharm Res. 2016;15(3):283.
11. Mercier F, Lefevre G, Huang HL, Truyen L, Snoeck E, Pinquier JL. Rivastigmine exposure provided by a transdermal patch versus capsules. Curr Med Res Opin. 2007;23(12):3199-204.
12. Cummings J, Lefevre G, Small G, Appel-Dingemanse S, Truyen L, Verhey F. Pharmacokinetic rationale for the rivastigmine patch. Neurology. 2007;69(4 Suppl 1):S10-3.
13. Blesa R, Truyen L, Devos T, Cummings J, Anand R, Vellas B. Caregiver preference for rivastigmine patches versus capsules for the treatment of Alzheimer disease. Neurology. 2007;69(4 Suppl 1):S23-8.
14. Mah K, Khan MA, Rahman A, Ali M, Ahmad S, Siddiqui Z. Muheet-e-Azam (Urdu translation). New Delhi: CCRUM; 2012.
15. Ghani KA, Advia Y, Khan MA, Rahman A, Ali M, Ahmad S. Idara Kitab al-Shifa. New Delhi; 2011:1260-1.
16. Sirohi B, Sagar R, Sharma A, Singh P, Kumar V, Gupta R. Effect of hydroalcoholic extract of Dactylorhiza hatagirea roots and Lavandula stoechas flower on thiopental sodium induced hypnosis in mice. J Drug Deliv Ther. 2019;9(4):414-7.

17. Mushtaq A, Khan RA, Ali N, Shah FA, Khan I, Ahmad S. Biomolecular evaluation of Lavandula stoechas L. for nootropic activity. Plants. 2021;10(6):1259.
18. Gilani AH, Aziz N, Khan MA, Shaheen F, Jabeen Q, Siddiqui BS. Ethnopharmacological evaluation of the anticonvulsant, sedative and antispasmodic activities of Lavandula stoechas L. J Ethnopharmacol. 2000;71(1-2):161-7.
19. Tayarani-Najaran Z, Emami SA, Asili J, Mirzaei H, Mousavi SH, Ghorbani A. Protective effects of Lavandula stoechas L. methanol extract against 6-OHDA-induced apoptosis in PC12 cells. J Ethnopharmacol. 2021;273:114023.
20. Ezzoubi Y, Chahdi FO, El Mousadik A, Benharref A, Jana M, Zaid A. Antioxidant and anti-inflammatory properties of ethanolic extract of Lavandula stoechas L. Int J Phytopharm. 2014;5(1):21-6.
21. Devi VK, Jain N, Valli KS, Prasad R, Singh M, Kumar A. Importance of novel drug delivery systems in herbal medicines. Phcog Rev. 2010;4(7):27.
22. Mustafa SB, Khan RA, Shah FA, Khan I, Ali N, Ahmad S. Antihyperglycemic activity of hydroalcoholic extracts of Curcuma longa, Lavandula stoechas, Aegle marmelos and Glycyrrhiza glabra and their polyherbal preparation in alloxan-induced diabetic mice. Dose Response. 2019;17(2):1559325819852503.
23. Al-Mariri A, Safi M, Ali A, Ahmad S, Khan MA, Rahman A. Antibacterial activity of selected Labiatae essential oils against Brucella melitensis. Iran J Med Sci. 2013;38(1):44.
24. Patel NA, Patel NJ, Patel RP, Patel DM, Patel GN, Patel KS. Design and evaluation of transdermal drug delivery system for curcumin as an anti-inflammatory drug. Drug Dev Ind Pharm. 2009;35(2):234-42.
25. Suksaeree J, Monton C, Madaka F, Chusut T, Pichayakorn W, Praphairaksit N. Formulation, physicochemical characterization and in vitro study of chitosan/HPMC blends-based herbal patches. AAPS PharmSciTech. 2015;16:171-81.
26. Latif MS, Abbas N, Zaman M, Khan MI, Khan MA, Ahmad S. Ethyl cellulose and hydroxypropyl methyl cellulose blended methotrexate-loaded transdermal patches: in vitro and ex vivo study. Polymers. 2021;13(20):3455.
27. Singh A, Bali A, Sharma S, Kumar P, Singh M, Gupta R. Formulation and characterization of transdermal patches for controlled delivery of duloxetine hydrochloride. J Anal Sci Technol. 2016;7(1):1-13.
28. Baviskar DT, Parik VB, Jain DJ, Sharma A, Singh P, Kumar V. Development of matrix-type transdermal delivery of lornoxicam: in vitro evaluation and pharmacodynamic and pharmacokinetic studies in albino rats. PDA J Pharm Sci Technol. 2013;67(1):9-22.
29. Ali FR, Khan MA, Ahmad S, Rahman A, Ali N, Shah FA. Design, development and optimization of dexibuprofen microemulsion-based transdermal reservoir patches for controlled drug delivery. Biomed Res Int. 2017;2017:1-10.
30. Salerno C, Carlucci AM, Bregni C, Gonzalez M, Ruiz A, Castro E. In vitro drug release and percutaneous absorption of fluconazole from topical dosage forms. AAPS PharmSciTech. 2010;11:986-93.
31. Latif MS, Abbas N, Zaman M, Khan MI, Khan MA, Ahmad S. Formulation and evaluation of hydrophilic polymer-based methotrexate patches: in vitro and in vivo characterization. Polymers. 2022;14(7):1310.
32. Suksaeree J, Monton C, Madaka F, Chusut T, Pichayakorn W, Praphairaksit N. Formulation of polyherbal patches based on polyvinyl alcohol and hydroxypropyl methyl cellulose: characterization and in vitro evaluation. AAPS PharmSciTech. 2017;18:2427-36.
33. Herman A, Herman AP, Nowak A, Zielinska A, Matysiak J, Kaczmarek M. Essential oils and their constituents as skin penetration enhancers for transdermal drug delivery: a review. J Pharm Pharmacol. 2015;67(4):473-85.